Malaysian Journal of Chemistry, 2025, Vol. 27(3), 602-612
(Special Issue: *International Conference on Sustainable Materials and Technologies, ICSMT 2025*)

A Novel Plasma Spray NiCr/Al_2O_3 and Cr_2C/ Al_2O_3 Coating Design for Hot Corrosion Prevention and to Enhance the Efficiency in Boiler Tubes

Somasundaram, B.[1]*, Vigneshkumar, M.[2], Kumar, R.[3], Muthusamy, P.[4], Raghunath, M.[5]* and Manivel, C.[6]

[1]Department of Mechanical Engineering, REVA University, Bengaluru, 560064 Karnataka, India
[2]Department of Mechanical Engineering, Sri Krishna College of Engineering and Technology, Coimbatore, 641008 Tamil Nadu, India
[3]Department of Mechanical Engineering, Ramaiah Institute of Technology, Bangalore, 560054 Karnataka, India
[4]Department of Mechanical Engineering, Pollachi Institute of Engineering and Technology, Coimbatore, 642205 Tamil Nadu, India
[5]Department of Mechatronics Engineering, Bannari Amman Institute of Technology, Erode, 638401 Tamil Nadu, India
[6]Department of Mechanical Engineering, NPR College of Engineering and Technology, Dindigul, 624401, Tamil Nadu, India
*Corresponding author (e-mail: somasundarb@reva.edu.in)

In the rigorous environment of boiler operations, corrosion harms the longevity and performance of crucial elements such as boiler tubes. To address this issue, the current work looks at the hot corrosion confrontation of Cr_2C and Ni-Cr based type of coatings applied through plasma spray in a replicated boiler environment. The coatings, which include NiCr /Al_2O_3 and Cr_2C /Al_2O_3, are applied to T22 steel substrates and extensively evaluated under circumstances that replicate the corrosive environment encountered during boiler operation. The efficiency of these coatings in preventing corrosion and maintaining the structural strength of T22 steel substrate is systematically evaluated using extensive analytical techniques such as corrosion testing, microscopy, and material characterization. The results show that NiCr and Cr_2C based coatings function well, with significant increases in corrosion resistance compared to uncoated substrates. Furthermore, the impact of composition of coating and microstructure on corrosion behaviour is examined, giving important information for the development of new corrosion-resistant materials for boiler applications. Overall, this work contributes to current efforts to improve boiler dependability, longevity, and operating efficiency by utilizing new coating methods.

Keywords: Hot corrosion; Thermogravimetric Analysis; thermal spraying; oxide scale

Received: February 2025; Accepted: May 2025

High temperature corrosion of metal building equipment in mutual gas environments containing compounds are potential problems for abundant fossil energy systems, in particular those that use coal as feedstock. Hot corrosion is initiate in numerous ways due to corroded products that differ in shape and turn into salty due to the high temperature. Steels and other materials go through a variety of working situations at high temperatures. Corrosion is an issue as a result of using steels in this high temperature application. Steels and other materials go through a variety of working situations at high temperatures. Corrosion is an issue as a result of using steels in this high temperature application. The oxidation of material at high temperatures is the main reason that allows boiler steel to corrode. The contaminants in the coal used in the boilers encompass oxide of vanadium, sodium, and sulphur. These contaminants combine with oxygen to form oxides, which can corrode metals [1]. Sulphur then combines with oxygen to form SO_2 and this SO_2 slightly oxidizes to form SO_3. When sodium and vanadium react with oxygen, they produce sodium and vanadium oxides. These oxides further combine to form multifaceted oxides of V and Na, which are popularly recognized as vanadate [2]. The term "heated rusting" refers to hot corrosion that has been accelerated because of salt [3]. Impurities such as V_2O_5 and NaCl combine to produce deposits which are molten that damage the protective coatings. In systems for producing energy, leftover fuel, oil and coal are frequently used due to the lack of high-quality fuels, as well as the reason for fiscal gain. These energies include contaminants that form composites on the material's surface at low melting points and will lead to decomposition. Such composites are usually named as Powder [4-6]. The supposed powder deposits on the physical exterior leads to hot decomposition. Substantial degeneration occurs when these liquefied composites liquefy the defensive oxide layers which are formed physically on the boiler tube materials

†Paper presented at the International Conference on Sustainable Materials and Technologies (ICSMT 2025)

during the operation of gas turbine [7-8]. Many situations that resulted in fatalities and property damage were due to a failure to prevent or minimally sense heated rusting at an initial phase. Tens of millions of dollars are frequently spent to restore deteriorated structures, machinery, and equipment adding up to the immediate expenses connected with shutdown and loss of productivity. Moreover, abrupt material degradation can result in human handicaps or even risk to life [9-10]. When boiler tubes and other parts are corroding, power plants may need to shut down. Boiler steam temperature and thermal efficiency are both reduced by corrosion.

Conventional steels, which are used extensively in thermal power plants, cannot tolerate corrosion issues. In recent years, scientists have enhanced the cyclic oxidation, erosion and high temperature hot corrosion protection of steel by using several types of coatings [11-12]. These days, a lot of items are coated using thermal spray technology to strengthen their resistance to abrasive wear and prolong their usable lives [13-14]. In recent years, these coatings have become more considerable significance to recover the Boiler steel life duration at high temperature environment applications. Inventions in the powder and wire production in addition to improvements made to heat-based spraying coating strategies have produced the expansion of external coatings with strong confrontation against weathering and corrosion. Such coating methods have no picky limitations in the core and surface composition [15-17]. The study found that the Cr_3C_2-NiCr coating was comparatively thick, consisting primarily of NiCr, Cr_3C_2 along with a small amount of Cr_7C_3. Composite coatings are applied to ASTM T22 steel in the present work, by adopting the HVOF technique and shown in Table 1. To the best of our knowledge, no prior research has reported on the improved high-temperature hot corrosion resistance of HVOF-sprayed composite coatings consisting of NiCr/Al_2O_3 and Cr_2C/Al_2O_3. The deprivation of T22 boiler bare steel is gradual when exposed to enhanced temperature engineering environments. To replicate these circumstances, we conducted trails using molten acidic salt (Na_2SO_4–60% V_2O_5) to evaluate the performance of both bare T22 steel and the previously mentioned coatings. This study aimed to compare the corrosion resistance of metal composite HVOF coatings containing either chromium oxide or silicon dioxide under heat treatment in molten salt conditions. Furthermore, our study involved a comprehensive evaluation of microscopic, structural, and weight-related changes in both uncoated and HVOF-coated specimens exposed to a high-temperature, molten salt-induced acidic corrosion environment.

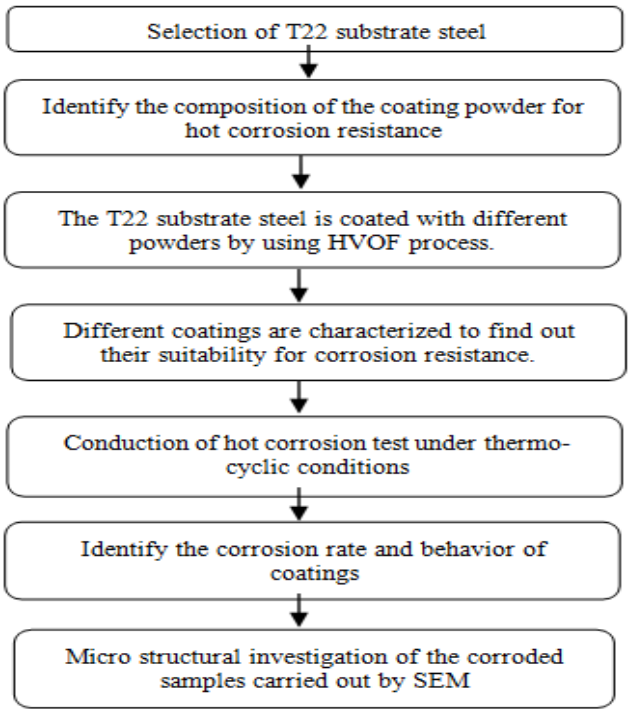

Figure 1. Methodology of coating process and characterization.

Now oxidative corrosion behaviour at increased temperature of the acidic molten salt mixture could worsen the T22 bare steel when exposed to corrosion. In addition, experiments were conducted to comprehend the relative outcome of chromium and silica oxides in the composite coating environment deposited by HVOF technique. HVOF and bare T22 steel samples were exposed to 700°C molten salt corrosion [18-20]. Weight gain, XRD, and SEM/EDS analyses revealed chromium oxide formation improved corrosion resistance, aiming to identify suitable protective coatings for high-temperature applications [21-22]. This study developed a reliable laboratory method to simulate hot corrosion, as outlined in Figure 1. It examines the corrosion behavior of HVOF-sprayed NiCr and Cr_3C_2 coatings on T22 steel under molten salt exposure, analyzing structural, microscopic, and weight changes. Bare and HVOF-coated samples were subjected to (Na_2SO_4–60%V_2O_5) molten salt at 700°C in thermocyclic conditions. Weight gain analysis and XRD/SEM-EDS characterization assessed corrosion. The study aims to identify effective coatings to protect uncoated T22 steel at high temperatures.

Latest advances in contemporary coating expertise resulted in numerous narrative coating compositions according to the necessities. In the scrupulous case where mutual high temperature corrosion and erosion resistance at superior temperature is essential, the relevance of Ni-based coatings received pervasive use. Ni-based coatings with alloying elements of chromium, silicon, molybdenum and other trivial elements have been tried. The present research is on developing NiCr/Al_2O_3 and Cr_2C/Al_2O_3 composite coatings with the accumulation of carbides and oxides and depositing using the HVOF process on bare alloy steel. The coatings are characterized and evaluated for its performance with respect to hot corrosion.

EXPERIMENTAL SECTION

Substrate Material

In the current study, uncoated T22 steel is selected as base uncoated material. Workpiece samples were cut as per ASTM standard of (SA213-T22) steel into square shapes (25×25×5) in mm for exposure testing. Prior to plasma spray coating, the specimens underwent grit blasting with aluminum oxide to enhance surface roughness. During coating, samples were fixed on rotating drum jigs using a turntable setup to achieve uniform deposition and minimize edge-related irregularities. Chemical composition of the T22 substrate steel mentioned in Table 1. On the T22 substrate steel, NiCr/Al_2O_3 and Cr_2C/Al_2O_3 composite coatings were applied using the plasma spray technique, with coating powders sized between 45 and 60 µm. Given that boiler construction involves steel tubes exposed to high temperatures, the parameters for plasma spray coating as mentioned in Table 2. Table 3 presents the weight percentage composition of the composite coatings. During the coating procedure, consistent spray parameters and a fixed spray distance were maintained. An average coating thickness of 200 µm was uniformly applied to all surfaces of the base metal. A finely roughened surface was created due to grit blasting aimed to increase adhesion involving the substrate and the coating. The composition and microstructure of the specimens were analyzed using Scanning Electron Microscopy (SEM) integrated with Energy Dispersive X-ray Analysis (EDAX), while phase identification of the coatings was carried out through X-ray Diffraction (XRD) analysis.

Table 1. The elemental composition of T22 substrate steel is presented in terms of weight percentage (wt%).

Fe	Cr	Mo	Mn	Si	C
Bal.	2.55	1.10	0.52	0.43	0.14

Table 2. The parameters utilized in the plasma spray process for coating application are detailed.

Process parameter of Plasma Spray Coating	Quantity in Units
Argon flow rate	300 l/min
Powder feed rate	35 g/min
Hydrogen flow rate	40-45 l/min
Hydrogen pressure	600 kPa
Nitrogen flow rate	500 l/min
Spray distance	200 mm
Argon pressure	900 kPa
Nitrogen pressure	550 kPa

Table 3. The chemical composition (wt%) of the composite coatings.

Plasma Coatings	Ni	Cr	Al	O	C
$NiCr/Al_2O_3$	39.9	15.4	2.1	4.9	-
$Cr2C/Al_2O_3$	-	39.9	15.4	4.9	3.5

Table 4. Changes in microhardness, coating thickness and porosity of samples coated using the HVOF method.

HVOF Coatings	Vickers Microhardness,VHN (GPa)	Coating Thickness(μm)	Porosity(%)
Cr_2C/Al_2O_3	814.3 HV 0.3	200	1.66
$NiCr/Al_2O_3$	801.9 HV 0.3	200	1.69

Coatings Characterization Techniques

The porosity property of the composite coatings was evaluated by means of an image analyzer (Metaplus software) following ASTM B276 guidelines. To assess the porosity of coated steel, the mean of eight measurements for each specimen was calculated. A cross-sectional micrograph of the composite coatings has been captured using a SEM. The Olympus bx53m upright metallurgical microscope, an inverted metallurgical microscope, was employed to assess the thickness of the coating. Microhardness measurements of the composite coatings were carried out using a Micro Vickers Hardness Tester (model VH1102) at Reva University, Bangalore. A load of 300 grams was applied, and readings were taken at eight different points along the cross-section of the coated sample. For surface characterization, the samples were sectioned, embedded in transoptic powder, and polished to a mirror finish using 0.3 μm diamond paste. Both coated and uncoated bare surfaces were examined with X-ray diffraction (XRD), using a diffractometer operated with CuKα radiation at 42 kV and 32 mA, scanning the samples over a 2θ range from 10° to 80°. SEM/EDAX analysis facilitated the characterization of the surface, composition at the cross-section of the sample, and morphology of both coated and uncoated specimens. Table 4 presents the changes in porosity, microhardness, and coating thickness of the samples coated using the HVOF method.

Recurring High-Temperature Corrosion Evaluation

Corrosion tests at high temperature were conducted in a molten salt (Na_2SO_4–60% V_2O_5) solution for 50 cycles under thermocyclic environment. Every cycle involved heating the samples in a furnace at 700°C for one hour, and then cooled at room temperature for twenty minutes. Figure 2 depicts the silicon carbide tube furnace. The experimental setup was chosen to mimic the environment seen in energy-producing machinery like boilers and furnaces. A Pt/Pt–13% Rh thermocouple was used to calibrate the silicon carbide tube heater, ensuring it remained within ±5°C of the specified temperature. Prior to testing, the samples' dimensions were meticulously measured using a vernier caliper to record their physical measurements. In contrast, specimens that were both naked and coated with plasma spray underwent hot corrosion testing. Prior to the corrosion test, the bare and coated specimens underwent wheel-cloth polishing with Al_2O_3 to achieve a mirror-like 1 ɛm finish. A systematic mixture of molten salt (Na_2SO_4–60% V_2O_5) and distilled water was prepared. The molten salt was evenly applied to preheated specimens at 250°C, with the coating thickness ranging from 3 to 5 mg/cm². The salt-coated samples were dried in an oven at 100°C for three to four hours. Before the high-temperature corrosion test, the dried, salt-coated samples were carefully placed in an alumina boat. Every specimen was placed into a crucible, and the combined weight of the specimen and the boat was recorded, noting any changes. Weight-change information was collected at the conclusion of each cycle. The corroded surfaces were visually inspected to document the scale's color, spalling and peeling. Post-corrosion, the surfaces of the specimens were examined using XRD and SEM/EDS methods for detailed analysis.

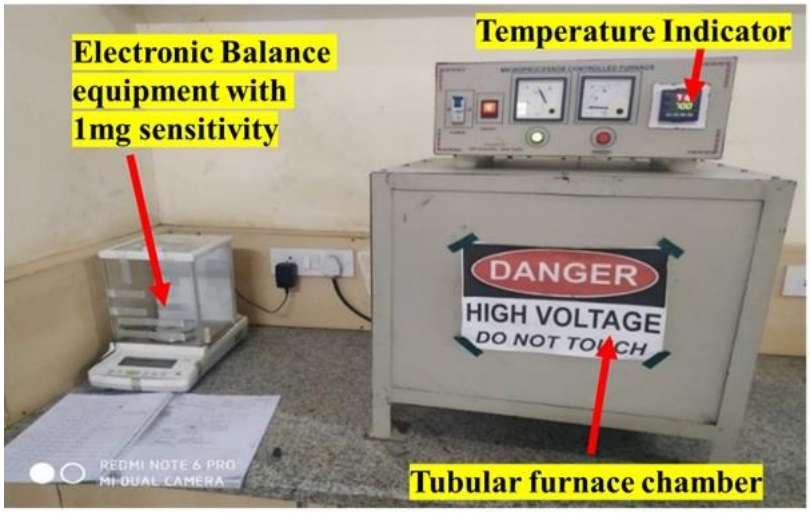

Figure 2. High Temperature Corrosion Experimental setup.

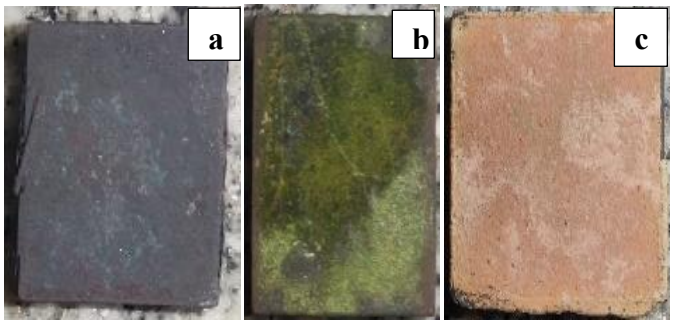

Figure 3. Macro images of the T22 substrate (uncoated) steel (a) and plasma-coated specimens, including NiCr/Al_2O_3 (b) and Cr_2C/Al_2O_3 (c), exposed to a Na_2SO_4–60%V_2O_5 environment at 700°C.

RESULTS AND DISCUSSIONS

In this present work, corrosion experiment has been conducted using the equipment as shown in Figure 2. Figures 3(a)–(c) illustrate the hot corrosion behavior of uncoated T22 steel, as well as NiCr/Al_2O_3 and Cr_2C/Al_2O_3 coated samples, when exposed to a molten salt environment. In the case of the uncoated T22 steel (Figure 4a), a dark grey oxide layer developed after the initial exposure cycle. This gradually transformed into a blackish-grey coating by the tenth cycle and remained relatively unchanged in subsequent cycles. The oxide layer on the unprotected T22 steel was observed to be brittle and showed signs of surface cracking. Early corrosion cycles also showed the oxide layer peeling off the T22 substrate. The NiCr/Al_2O_3-coated sample (Figure 4b) exhibited a light brown color by the 10th cycle, which remained consistent through the 50th cycle. The Cr_2C/Al_2O_3-coated sample (Figure 4c) transitioned from dark grey to a greenish tint by the 10th cycle, maintaining this color until the end of the corrosion assessment. Throughout high-temperature corrosion assessment, the composite coatings showed no significant signs of spalling, peeling, or cracking.

Kinetics of Corrosion in Molten Salt

Figure 4 (a) illustrates the weight change per unit area of cycles for T22 steel and the NiCr/Al_2O_3 and Cr_2C/Al_2O_3 composite coatings subjected to thermocyclic hot corrosion treatment. The weight growth in T22 substrate steel increases quickly to the tenth cycle. Weight increase is seen when it keeps rising till 55 cycles. Then overall change in weight of corroded samples at molten acidic salt environment is influenced by both the weight gain from oxide scale formation and the weight loss due to possible fluxing and spalling of oxide layers. The T22 (substrate steel) showed greater weight variation compared to the composite coatings. Figure 4 (b) presents a plot of (weight change/area)² vs the number of cycles for both the coated and uncoated specimens. The graph indicates that composite coatings adhered to the parabolic rate law, whereas T22 steel showed minor departures from it. T22 substrate steel exhibited a greater weight gain than the Cr_2C/Al_2O_3 and NiCr/Al_2O_3 composite coatings, owing to the creation of a thick oxide scale as a result of the composite coatings' chemical reaction. It is made clear by Figure 4 (c) that in a heated corrosion environment, both

coated and uncoated bare specimens follow the Parabolic Rate Law (PRL). Equation (1), which represents the investigational relationship of the PRL, yields kp.

$$(\Delta W/A)^2 = kp \times t \quad (1)$$

In this above Equation (1), ΔW indicates the variation in the weight of T22 steel from its original value, A corresponds to the surface area, and t represents the duration of oxidation measured in seconds. Figure 4 (d) shows that cumulative weight gain plot. According to the cumulative weight gain, the corrosion resistance of the samples is ranked as follows: Bare T22 steel ≥ NiCr/Al_2O_3 coated steel ≥ Cr_2C/Al_2O_3 coated steel. The kp values and cumulative weight gain for both the coated and bare specimens as tabulated in Table 5.

Table 5. kp and total weight gain values.

Samples	kp $g^2/cm^4/s^1$	Cumulative Weightgain (mg/ cm^2)
T22 substrate steel	6.383×10^{-9}	18.204
NiCr/Al2O3	9.2869×10^{-11}	3.94
Cr2C/AL2O3 coating	1.7972×10^{-11}	3.74

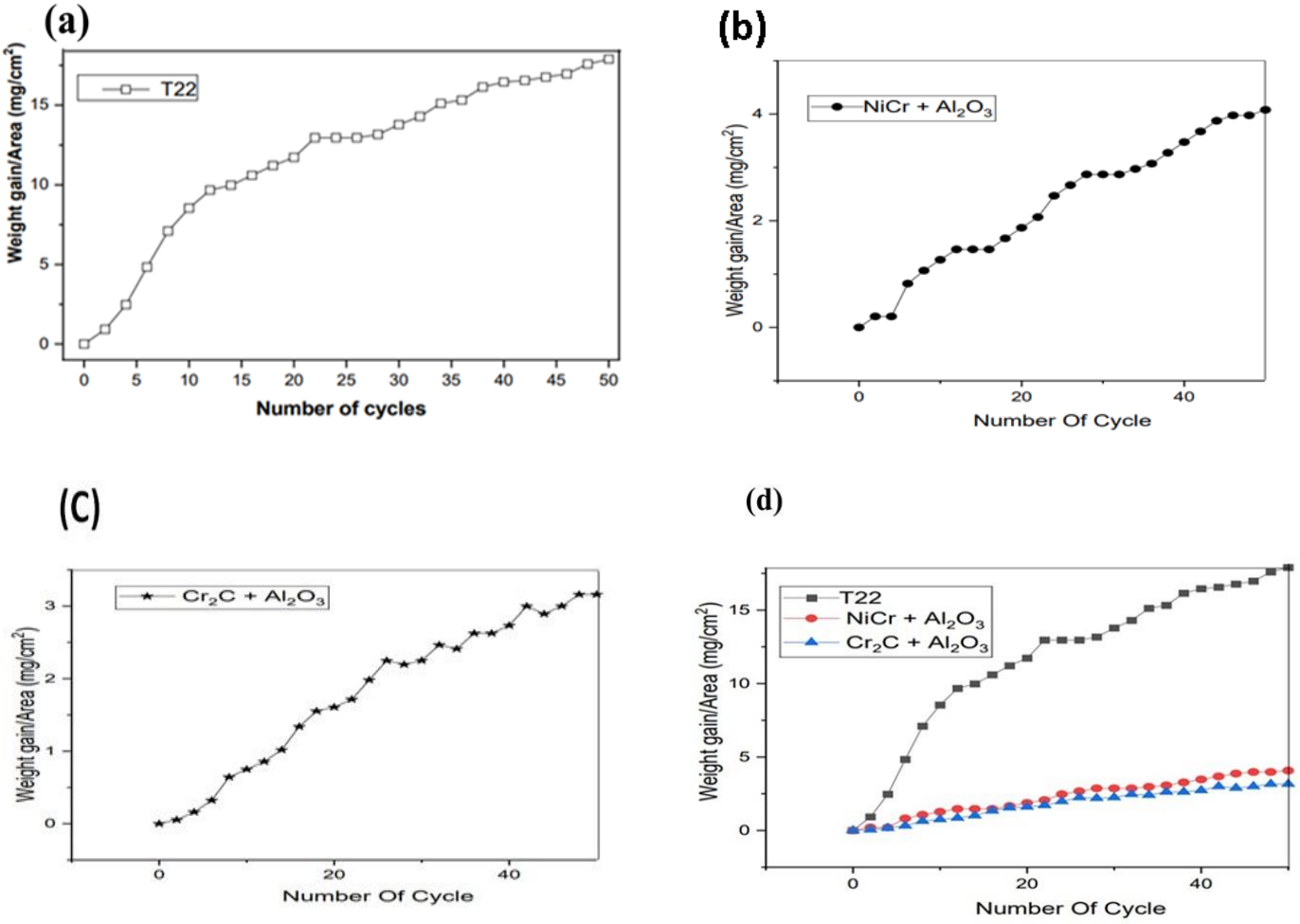

Figure 4. (Weight change per unit area) versus the number of cycles for (a) T22 steel, (b) NiCr + Al_2O_3 coated steel, (c) Cr_2C + Al_2O_3 coated steel, and (d) both uncoated and coated steels.

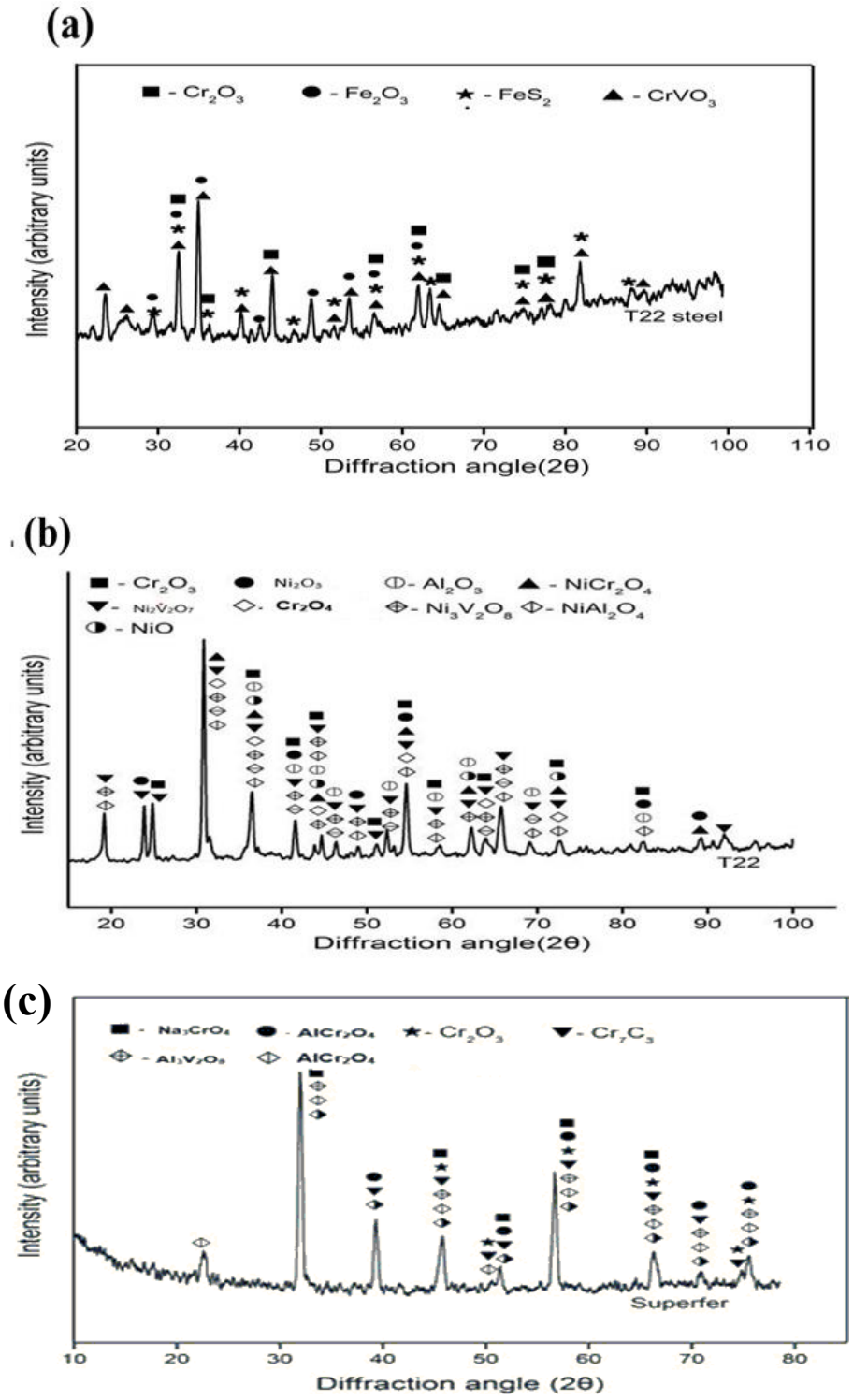

Figure 5. XRD spectra for (a) uncoated T22 substrate steel and plasma-sprayed (b) NiCr/Al_2O_3 and (c) Cr_2C/Al_2O_3 specimens subjected to hot corrosion at 700°C.

XRD Analysis of Oxide Phases

The XRD patterns illustrating the phases present in the oxide scales of hot-corroded T22 bare substrate steel and composite coatings are shown in Figures 5 (a-c). As shown in Figure 5 (a), The oxide scale formed on the uncoated T22 steel predominantly consists of Fe_2O_3, with smaller amounts of phases like Cr_2S_3, $NaVO_3$, and NaV_2O_5 also present. Figure 5 (b) shows that the NiCrMoFeCoAl-30%SiO_2 composite coating contains primary phases such as SiO_2, Al_2SiO_5, $CoSi_2$, Al_2O_3, and $Cr_2(SO_4)_3$, along with secondary phases like Fe_2SiO_4, $FeVO_4$, and Cr_3Si. In Figure 5 (c), the NiCrMoFeCoAl-30%Cr_2O_3 composite coating exhibits

major phases including Cr_2O_3, $NaVO_3$, and $NiCr_2O_4$, with minor phases like $AlFeO_3$ and Co_3Fe_7. The creation of metal chromites and chromates at elevated temperatures could contribute to improved corrosion resistance.

SEM/EDS Analysis of the Oxide Scales

Figures 6(a–c) present SEM/EDS micrographs that reveal the surface morphology of both the uncoated T22 steel and the plasma-sprayed composite coatings after exposure to hot corrosion. EDS was performed on targeted areas and specific points across the corroded surfaces. The oxide layer on the bare T22 steel was characterized by a rough surface appearance and the presence of dark spots, scale spalling, and signs of bulge. EDS analysis showed that the T22 substrate steel primarily consisted of Fe_2O_3, with smaller amounts of NiO, V_2O_5, Cr_2O_3, and SiO_2 detected at EDS spot 1. The scales observed in selected area 1 (Figure 6a) contained Fe_2O_3, Al_2O_3, and MnOx.

The oxide scale of hematite (Fe_2O_3) identified as less protective in previous studies on superheater tubes experiencing fireside corrosion failures. Figure 6 (b) shows the SEM/EDS images of the outside morphology of the NiCr/Al_2O_3 coated composite specimen, revealing the occurrence of Al_2O_3, Cr_2O_3, and SiO_2 at EDS spot 1. Additionally, Mo_2O_3, Al_2O_3, and SiO_2, Fe_2O_3 scales are observed in selected area 1. For the Cr_2C/Al_2O_3 composite coated specimen (Figure 6c), the oxide scale exhibited a substantial structure, predominantly consisting of Cr_2O_3 and V_2O_5, with NiO and Na_2O detected in selected area 1 and Cr_2O_3, Na_2O, V_2O_5, and Al_2O_3 noted at EDS spot 1. The oxide scales on the coated specimens formed dense, continuous, and uniform clusters, showing no spallation or cracking. Both XRD and EDS analyses confirmed the presence of Cr_2O_3, Na_2O, SiO_2, and Al_2O_3 phases.

The combined findings from microscopic, gravimetric, and structural analyses indicate progressive corrosion of the uncoated T22 substrate steel, leading to significant degradation in molten salt conditions. The uncoated T22 exhibited the highest weight gain, while the Cr_2C-containing coating showed the lowest weight gain. High-temperature effects combined with Na_2SO_4-60% V_2O_5 intensify the oxidative processes affecting uncoated T22 substrate steel. Nevertheless, both of the plasma coatings demonstrated enhanced stability in terms of gain in weight kinetics. Thermogravimetric analysis emphasizes the accelerated corrosion kinetics caused by the Na_2SO_4-60% V_2O_5 eutectic mixture. Then further supported by the detection of additional metal oxides in the XRD and SEM/EDS analyses.

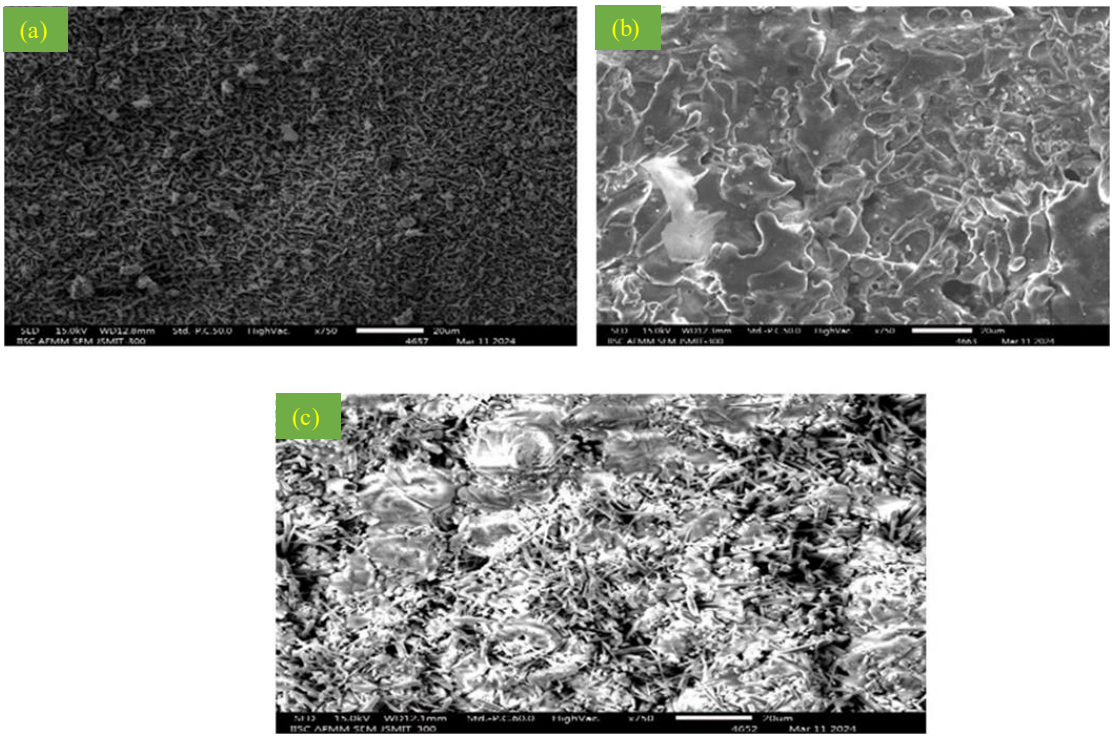

Figure 6 (a-c). Surface analysis using SEM/EDS was conducted on both bare and coated specimens after exposure to hot corrosion.

The presence of high-valent metal ions, combined with the melted molten salt mixture on the T22 surface, can lead to increased local acidity. This, in turn, may cause the protective oxides to flux acidically, resulting in a additional scale of porous oxide that allows violent gaseous mixtures to arrive at the base substrate metal at elevated temperatures. The sizzling corrosion kinetics of NiCr/Al_2O_3 coated steel exhibited a parabolic trend. The oxides SiO_2, Mo_2O_3, and V_2O_5 formed. Additionally, these oxides have similar coefficients of thermal expansion, which helps minimize thermal stresses. The scales of oxide on the coated steel are dense and adherent, showing no spalling or cracking. These oxide scales protect alloy, with the coatings' resistance to scale spalling primarily influencing their repeated oxidation behavior. The enhanced hot corrosion resistance of Cr_2C/Al_2O_3 protects oxides layer on the surface.

The outermost film of the oxide scale primarily consists of Cr and Al oxides and spinels, which exhibit low solubility in the highly acidic Na_2SO_4-60% V_2O_5 molten melt. The oxides developed form a barricade that prevents the dissemination of O_2 and corrosion from the molten salt addicted to the underlying coating, thus keeping the region underneath the oxide scale. The gradual oxidation behavior and the parabolic trend observed in the gravimetric analysis indicate that the process is diffusion-controlled. In the initial stages of hot corrosion, the development of chromium-based oxides serves as a protective barrier against further degradation, preventing the more rapid oxidation of nickel and chromium. The protective nature of the refractory environment surrounding nickel and chromium helps maintain the structural integrity of the coating, preserving its mechanical properties. The hot-corroded plasma-sprayed Cr2O3 coating promotes the formation of a denser and less porous structure compared to the SiO2 coating. This increased density provides better protection for the T22 steel substrate against corrosive elements at elevated temperatures. These observations support the superior corrosion resistance of the Cr2O3/Al2O3 coating over the SiO2-based composite coating.

The cumulative findings from microstructural, cyclic, and high-temperature corrosion analyses indicate a gradual but significant deterioration of uncoated T22 steel when exposed to molten salt environments. The porous nature of the corrosion products facilitates further ingress of corrosive agents, accelerating the degradation process. The presence of a Na_2SO_4–60% V_2O_5 salt mixture at elevated temperatures intensifies oxidation, exacerbating material loss in the uncoated steel. In contrast, High Velocity Oxy-Fuel (HVOF) sprayed coatings demonstrate superior resistance, as evidenced by their more favorable weight gain behavior during kinetic assessments.

The analysis of cyclic hot corrosion data aims to uncover the corrosion kinetics driven by the Na_2SO_4-60%V_2O_5 eutectic mixture. The oxide layer formed on the exposed T22 steel predominantly consists of iron oxide, which governs the hot corrosion rate of the steel. This corrosion process is further influenced by the presence of additional metal oxides, which have been identified through SEM/EDS and XRD analyses.

The presence of higher-valence metal ions can intensify localized acidity in combination with the molten salt mixture on the bare T22 steel substrate. This condition may promote acidic fluxing of protective oxide layers, leading to the formation of a more porous oxide scale. Such porosity enhances the penetration of aggressive gases to the underlying metal at elevated temperatures. The formation of oxides on outer surface exhibited closely matched coefficients of thermal expansion, which helps in minimizing thermal stress during high-temperature exposure. On HVOF-coated steel, the resulting oxide scales are compact, adherent, and free from cracking or spallation. These dense scales serve as effective barriers, providing robust protection to the underlying alloy. The resistance to scale spallation is a key factor governing the cyclic oxidation performance of all HVOF-applied coatings. The outermost oxide layer is primarily composed of chromium and nickel oxides, along with their spinel forms, which exhibit low solubility in the highly acidic Na_2SO_4–60% V_2O_5 molten salt environment.

The formation of oxides serves as barrier, limiting diffusion of oxygen and molten salt products into coating, thus preventing further oxidation beneath the oxide layer. The slow oxidation kinetics and parabolic behavior observed in cyclic hot corrosion tests indicate that the reaction rate is diffusion-controlled. The refractory properties of nickel and chromium help maintain the coating's mechanical strength. Additionally, the hot-corroded composite coating generates metal chromites, chromates, and oxides, which enhance its resistance to further corrosion. This effectively shields the bare T22 steel substrate from the penetration of corrosive species at elevated temperatures.

The literature evaluation highlights the significant efforts made to alleviate hot corrosion in coal-fired boilers and to better comprehend the process of alloy degradation. Progress has been achieved on both fronts, even though in many cases where corrosion-erosion challenges are encountered in boiler tube materials, altering the alloy composition is not always a viable solution due to potential losses in desired mechanical properties. As a result, the development of improved corrosion-resistant coatings for fundamentally unaltered alloys is significant. These coatings have to offer protection against mutually corrosion and erosion concurrently. Lately, HVOF composite coatings, which integrate carbides and oxide-forming agents dispersed in a long-lasting matrix, have been recognized as a talented approach.

These coatings are intended to endure aggressive high-temperature environments with multifaceted gas compositions. Similar to the developed coatings for boiler tubes, the novel plasma spray coatings offer hot corrosion resistance, enhancing the robustness and efficacy of heat pump water tanks under dynamic thermal stress [23-25]. Furthermore, it is not only necessary to create and evaluate new coatings but also to fully understand their performance and the principal mechanisms of degradation in the ruthless corrosion conditions characteristically found in boiler systems.

CONCLUSIONS

In the present study, composite coatings were applied to uncoated bare substrate T22 steel, and their high-temperature corrosion behavior is investigated. The observed conclusions are drawn as follows: Composite Coating Application: The Cr_2C/Al_2O_3 and NiCr/Al_2O_3 composite coatings were successfully deposited on T22 substrate steel using the plasma spray process, achieving a coating thickness of approximately 200 µm. Corrosion Performance: The uncoated T22 steel was subjected to significant scale peeling, severe spalling, and considerable weight gain. In contrast, the weight gains for Cr_2C/Al_2O_3 and NiCr/Al_2O_3 coated specimens were 88.17% and 96.84% lower, respectively, compared to the uncoated T22 steel when exposed to a molten salt environment at 700°C under thermocyclic conditions. Phase Composition: For Cr_2C/Al_2O_3 coated T22 steel, Cr_2O_3 was identified as the primary phase, while NiCr/Al_2O_3 coated T22 steel primarily contained Al_2O_3 and NiO. These findings were confirmed through SEM/EDS and XRD analyses in the molten salt environment at 700°C. Corrosion Resistance: The hot corrosion resistance of the composite coatings was superior to that of the uncoated substrate. The hot corrosion resistance of the specimens ranked as follows: Cr_2C/Al_2O_3 coating > NiCr/Al_2O_3 coating > T22 substrate steel. The Cr_2C/Al_2O_3 plasma composite coating demonstrated better stability compared to the silica-based composite when exposed to high temperature.

REFERENCES

1. Rapp, R. A. and Zhang, Y. S. (1994) Hot corrosion of materials: fundamental studies. *The Journal of The Minerals, Metals & Materials Society*, **46**, 47–55.

2. Srikanth, S., Ravikumar, B., Das, S. K., Gopalakrishna, K., Nandakumar, K. & Vijayan, P. (2003) Analysis of failures in boiler tubes due to fireside corrosion in a waste heat recovery boiler. *Engineering Failure Analysis*, **10(1)**, 59–66.

3. Eliaz, N., Shemesh, G. & Latanision, R. M. (2002) Hot corrosion in gas turbine components. *Engineering Failure Analysis*, **9(1)**, 31–43.

4. Kamal, S., Jayaganthan, R., Prakash, S. (2009) Evaluation of cyclic hot corrosion behaviour of detonation gun sprayed Cr3C2–25%NiCr coatings on nickel- and iron-based superalloys. *Surface and Coatings Technology*, **203**, 1004–1013.

5. Sidhu, V. P. S., Goyal, K., Goyal, R. (2019) Hot corrosion behaviour of HVOF-sprayed 93 (WC-Cr3C2)-7Ni and 83WC-17Co coatings on boiler tube steel in coal fired boiler. *Australian Journal of Mechanical Engineering*, **17(2)**, 127–132.

6. Singh, G., Bala, N., Chawla, V. (2020) Microstructural analysis and hot corrosion behavior of HVOF-sprayed Ni-22Cr-10Al-1Y and Ni-22Cr-10Al-1Y-SiC (N) coatings on ASTM-SA213-T22 steel. *International Journal of Minerals, Metallurgy and Materials*, **27(3)**, 401–416.

7. Ramesh, M. R., Prakash, S., Nath, S. K., Sapra, P. K., Venkataraman, B. (2010) Solid particle erosion of HVOF sprayed WC-Co/NiCrFeSiB coatings. *Wear*, **269(3-4)**, 197–205.

8. Sidhu, H. S., Sidhu, B. S., Prakash, S. (2006) Mechanical and microstructural properties of HVOF sprayed WCCo and Cr3C2-NiCr coatings on the boiler tube steels using LPG as the fuel gas. *Journal of Materials Processing Technology*, **171(1)**, 77–82.

9. Uusitalo, M. S., Vuoristo, P. M. J., Mäntylä, T. A. (2003) High temperature corrosion of scoating sand boiler steels in oxidizing chlorine-containing atmosphere. *Materials Science and Engineering: A*, **346(1-2)**, 168–177.

10. Sivakumar, R., Joshi, S. V. (1991) Protective Coatings by Plasma Spraying: A Review. *Transactions of the Indian Ceramic Society*, **50(1)**, 1–14.

11. Kumar, S., Bhatia, R., Singh, H. (2020) Hot Corrosion Behaviour of CNT Reinforced Zirconium Yttrium Coatings in Molten Salt Environment. *Journal of Bio- and Tribo-Corrosion*, **6**, 81.

12. Goyal, K., Goyal, R. (2020) Improving hot corrosion resistance of Cr3C2–20NiCr coatings with CNT reinforcements. *Surface Engineering and Applied Electrochemistry*, **36(11)**, 1200–1209.

13. Mahajan, S., Chhibber, R. (2019) Hot Corrosion Study of 9Cr-1Mo Boiler Steel Exposed to Different Molten Salt Mixtures. *Transactions of the Indian Institute of Metals*, **72(9)**, 2329– 2348.

14. Sidhu, Buta Singh, Puri, D. and Prakash, S. (2004) Characterisations of plasma sprayed and

laser remelted NiCrAlY bond coats and Ni3Al coatings on boiler tube steels. *Materials Science and Engineering: A*, **368.1-2**, 149–158.

15. Gond, D., Chawla, V., Puri, D. and Prakash, S. (2010) High temperature corrosion behaviour of T-91 and T-22 bare steel in 75wt.% Na 2 SO 4+ 25wt.% NaCl molten salt environment at 900 C. *Journal of Minerals and Materials Characterization and Engineering*, **9(07)**, 593.

16. Oksa, Maria, Tommi Varis and Kimmo Ruusuvuori (2014) Performance testing of iron based thermally sprayed HVOF coatings in a biomass-fired fluidised bed boiler. *Surface and Coatings Technology*, **251**, 191–200.

17. Kumar, S., Bhatia, R. and Singh, H. (2020) Hot corrosion behaviour of CNT reinforced zirconium yttrium coatings in molten salt environment. *Journal of Bio-and Tribo-Corrosion*, **6(3)**, 81.

18. Kumar, K., Kumar, S. and Gill, H. S. (2023) Role of Surface Modification Techniques to Prevent Failure of Components Subjected to the Fireside of Boilers. *Journal of Failure Analysis and Prevention*, **23**, 1–15.

19. Singh, V., Singla, A. K., Bansal, A. (2023) Enhanced erosion resistance of HVOF-deposited laser-textured TiC coating with PTFE. *Surface Engineering*, **39(7-12)**, 816–822.

20. Yadav, A. S., Mishra, S. B. (2024) Comparative erosion performance of HVOF and LVOF sprayed NiCrSiBCFe-WC-Co coating. *Surface Engineering*, **40(5)**, 575–590.

21. Agnihotri, A., Vasudev, H. and Singh, G. (2025) Evaluation of HVOF Sprayed and Burnished WC-Co-Cr Coatings on Boiler Steel: Mechanical and Microstructural Properties. *Journal of Bio- and Tribo-Corrosion*, **11**, 50.

22. Singh, V., Kumar, V., Bansal, A., et al. (2024) Investigating the Effect of Poly-tetra-fluoro-ethylene on the Cavitation-Erosion and Corrosion Resistance of HVOF Sprayed TiC Coatings on Stainless Steel. *Journal of Materials Engineering and Performance*, **33**, 12990–13003.

23. Chinnasamy, S., Prakash, K. B. Divyabharathi, R., Kalidasan, B., Rajamony, R. K., Pandey, A. K., Fouad, Y. and Soudagar, M. E. M. (2024) Performance and feasibility study of a heat pump with modified solar-air source evaporator: Techno-economic analysis for water heating. *International Communications in Heat and Mass Transfer*, **157**, 107795.

24. Chinnasamy, S., Prakash, K. B., Kalidasan, B. and Sampathkumar, A. (2024) Solar-air source heat pump water heater for scorching climatic condition: energy, exergy, economic and enviro economic (4E) exploration for sustainable future. *Applied Thermal Engineering*, **240**, 122212.

25. Chinnasamy, S., Prakash, K. B., Kalidasan, B. and Sampathkumar, A. (2024) Optimal utilisation of low-grade solar-air source for heat pump water heating using a dual-source evaporator with forced convection. *International Communications in Heat and Mass Transfer*, **150**, 107174.